Data envelope fitting with constrained polynomial splines

Abdelaati Daouia[a], Hohsuk Noh[b] and Byeong U. Park[c]

[a] Institute of Statistics, Université catholique de Louvain, Belgium
& Toulouse School of Economics, University of Toulouse, France
(abdelaati.daouia@tse-fr.eu)
[b] Department of Statistics, Sookmyung Women's University, South Korea
(word5810@gmail.com)
[c] Department of Statistics, Seoul National University, South Korea
(bupark@stats.snu.ac.kr)

Abstract

Estimation of support frontiers and boundaries often involves monotone and/or concave edge data smoothing. This estimation problem arises in various unrelated contexts, such as optimal cost and production assessments in econometrics and master curve prediction in the reliability programs of nuclear reactors. Very few constrained estimators of the support boundary of a bivariate distribution have been introduced in the literature. They are based on simple envelopment techniques which often suffer from lack of precision and smoothness. Combining the edge estimation idea of Hall, Park and Stern with the quadratic spline smoothing method of He and Shi, we develop a novel constrained fit of the boundary curve which benefits from the smoothness of spline approximation and the computational efficiency of linear programs. Using cubic splines is also feasible and more attractive under multiple shape constraints; computing the optimal spline smoother is then formulated into a second-order cone programming problem. Both constrained quadratic and cubic spline frontiers have a similar level of computational complexity to the unconstrained fits and inherit their asymptotic properties. The utility of this method is illustrated through applications to some real datasets and simulation evidence is also presented to show its superiority over the best known methods.

1   Introduction

Frontier modeling—that is, estimating the topological extremity of the support of a bivariate density function—is one of the basic tools in statistical applications. This has been well reflected by the expanding recent literature on data edge and data envelope analysis. A number of semi- and non-parametric techniques have been proposed, including extreme

values (de Haan and Resnick (1994), Hall *et al.* (1997), Gijbels and Peng (2000), and Girard and Jacob (2003, 2004)), projections (*e.g.* Jacob and Suquet (1995)), piecewise polynomials (Härdle *et al.* (1995), and Korostelev and Tsybakov (1993)), or local polynomials (Hall and Park (2004), Hall *et al.* (1998), and Knight (2001)).

In this article we focus on the less-discussed problem of estimating boundary curves that are believed or required to be monotone. This problem has increasing usage in classification and cluster analysis, economics, education, finance, management, physics, public policy, and other arenas. It is also closely related to edge estimation in image reconstruction. A first application that we consider in this article is concerned with the reliability of nuclear reactors. An accurate knowledge of the change in fracture toughness of the reactor pressure vessel materials as a function of the temperature is of prime importance in a nuclear power plant lifetime program. Physical considerations lead to the natural assumption that the master curve prediction—that is, the set of materials having optimal fracture toughness—is monotonely increasing. The scatterplot of 254 non-irradiated representative steels, obtained from the US Electric Power Research Institute (EPRI), is given in Figure 1 (left panel).

Our second motivating example is concerned with the increase of the production activity of 123 American electric utility companies. The measurements for each company of the produced output and the total cost involved in the production are represented in Figure 1 (middle panel). Naturally, the econometric frontier—that is, the locus of the most efficient firms—is nondecreasing. Another related application is concerned with the assessment of the efficiency of 37 European Air Controllers. The performance of each controller can be measured by its "distance" from the efficient support boundary, called cost/production frontier. The scatterplot of the controllers in the year 2000 is given in Figure 1 (right panel), where their activity is described by one input (an aggregate factor of different kind of labor) and one output (an aggregate factor of the activity produced, based on the number of air movements controlled, the number flight hours controlled, etc.).

Most of the works on boundary curve estimation do not rely on the monotonicity constraint and require large samples to provide good results. There are mainly two known methods for preserving monotonicity: the free disposal hull (FDH) and the data envelopment analysis (DEA). The FDH estimator is the lowest "stair-case" monotone curve covering all the data points (see, *e.g.*, Korostelev *et al.* (1995)). When the joint support is in addition convex, the DEA estimator is defined as the least concave majorant of the FDH frontier (see, *e.g.*, Gijbels *et al.* (1999)). Although FDH and DEA estimators are very simple in nature, their full statistical aspects have been elucidated only during the last decade. See, for instance, Jeong and Park (2006), Kneip *et al.* (2008), Daouia *et al.* (2010) and Park *et al.* (2010) for recent contributions. An improved version of the FDH estimator, referred

2

to as the linearized FDH (LFDH) and obtained by drawing the polygonal line smoothing the staircase FDH curve, has been considered in Hall and Park (2002) and Jeong and Simar (2006).

Although the FDH, LFDH and DEA estimators are very easy to implement and provide the fitted values at the observed predictor with monotonicity, they undersmooth the data and underestimate the true support boundary. These vexing defects are more exacerbated in case of small samples as those explored in our applications. Typically, the development of the asymptotic theory of these estimators requires the assumption that the unknown frontier function, φ, is at least continuously differentiable. It is then natural to incorporate such information into the estimation procedure. The idea of this paper is to combine spline smoothing with monotonic boundary estimation. It is well known that φ and φ' can be uniformly approximated by polynomial splines and their derivatives (see, *e.g.*, Dierckx (1993) and Schumaker (2007)). We propose to estimate the data edge with a monotone spline function defined on a suitably chosen set of knots, which envelopes the full data and minimizes the area under its graph. A similar idea can be found in Hall, Park and Stern (1998), where the boundary curve is rather modeled by a single polynomial of known degree, and without the inherent monotonicity constraint. The argument of polynomial approximation is very attractive in terms of both pragmatic and didactic advantages. Spline functions extend the advantages of polynomials to have greater flexibility as they are piecewise polynomials with specified continuity constraints. They also afford the possibility of imposing monotonicity and addressing a wide variety of settings, especially the range of applications which are likely to have non-polynomial boundary curves.

The first proposed estimator in this work is derived by minimizing the integration of a polynomial spline, and both monotonicity and data envelopment can be characterized by linear constraints. In this way, the minimization problem can be efficiently solved by a very simple linear programming algorithm. A similar estimator was considered in the context of regression smoothing with monotonicity by He and Shi (1998), who suggested using a constrained least absolute deviation principle in the space of polynomial splines to impose monotonicity. Our approach is different from theirs at least in the following two important aspects: it has the additional data envelopment constraint and its optimization criterion is the integration of splines rather than the L_1-type loss function. However, we share with He and Shi the elegant idea of using quadratic splines on a selected knot mesh to impose monotone constraint efficiently. Higher-order splines are more appealing for smoothness, but monotonicity can no longer be characterized as linear constraints at the knots.

Yet, using cubic splines to estimate a smooth monotone support boundary is also possible. The key argument is that the necessary and sufficient condition for a cubic spline

3

smoother to be nondecreasing can be characterized as second-order cone constraints. The envelopment constraint remains a linear one, and hence is a second-order cone constraint as well. Therefore, the estimation of the unknown parameters can be formulated into a standard second-order conic programming problem. This method inherits the attractive properties of cubic spline approximations and the computational efficiency of convex optimization. We refer to Alizadeh and Goldfarb (2003) for an influential paper in the second-order cone programming (SOCP) literature. In statistics, there is very little literature on the use of SOCP for estimation and inference purposes. Up to our knowledge, only Wang and Li (2008) have used SOCP for isotonic smoothing spline regression, and Papp and Alizadeh (2013) have suggested recently to apply this technique in a more general manner to some shape constrained estimation problems including density and regression estimation.

The choice of the number and location of knots for regularizing both estimated quadratic and cubic spline functions is a major issue in practice, but the shape constraint makes this selection easier than the unconstrained smoothing problem. Indeed, as monotonicity reduces sharp changes in the slope and curvature of the estimated frontier, typically a very small number of knots will suffice for the success of our methods. An adequate set of knots can be determined by analogy to the popular Akaike information criterion (AIC) and Bayesian information criterion (BIC). Both these selection criteria work remarkably well as demonstrated in various simulated scenarios in Section 4.

In some applications, concavity is also an important characteristic of the monotone function being fitted. For example, this naturally occurs when analyzing production performance of firms in a variety of industries. Aside from our motivating applications in the production setting, the problem of estimating concave monotone boundaries also naturally appears to be useful in portfolio management. In capital asset pricing models (CAPM), the volatility or the variance of a portfolio and its average return are analogous to input and output in models of production; the upper boundary of the attainable set of portfolios gives a benchmark relative to which the efficiency of an investment portfolio can be measured (see, *e.g.*, Gijbels *et al.* (1999) and the references therein). Such examples are abundant in economics and related fields. Both linear and second-order cone programming problems can easily be expanded to include the additional concavity constraints that are linear. This is much harder to do with other methods except for the piecewise linear DEA approach.

Section 2 describes in detail the constrained quadratic and cubic spline smoothing methods, including computation via linear programming and second-order cone programming as well as knot selection processes. Section 3 presents some indicative rates of strong uniform convergence for the unconstrained frontier estimates. We show that the monotone quadratic spline fit inherits the asymptotic rate of its unrestricted version, and the same holds true

for the cubic spline fit under both separate and simultaneous monotonicity and concavity constraints. Section 4 provides a comparison with the best known frontier estimation methods through Monte Carlo experiments. Section 5 returns to our motivating applications and illustrates the utility of the spline smoothing for the reliability of nuclear reactors and the performance of air controllers and electric utility companies. Section 6 concludes and the Appendix provides necessary mathematical proofs.

2 Constrained Polynomial Spline Smoothing

Suppose that we have n pairs of observations (x_i, y_i), $i = 1, \ldots, n$, from a bivariate distribution with a density $f(x, y)$ in $\mathbb{R}^2$. The support Ψ of f is assumed to be of the form

$$
\begin{aligned}
\Psi = \{(x,y)|y \le \varphi(x)\} &\supseteq \{(x,y)|f(x,y) > 0\}, \qquad (1)\\
\{(x,y)|y > \varphi(x)\} &\subseteq \{(x,y)|f(x,y) = 0\},
\end{aligned}
$$

where φ is a monotone increasing and/or concave function whose graph corresponds to the locus of the curve above which the density f is zero. Without much loss of generality, we restrict ourselves to $x_i \in [0, 1]$ and $y_i \ge 0$. We are interested in estimating φ based on the sample $\{(x_i, y_i), \ i = 1, \ldots, n\}$ by making use of its spline approximation.

A quadratic spline smoother of φ can easily be defined using either the B-spline basis or the truncated power function basis. In Section 2.1, we only describe the definition based on the more popular B-spline basis, which is known to have the desired computational convenience due to the sparsity of the design matrix. In spite of the computational expedience of the resulting B-spline estimator using linear programming, revealing its asymptotic properties is a tedious matter in the case of multiple shape constraints because of the discontinuity at knots of the second derivatives of the underlying piecewise quadratic polynomials. Making use of cubic splines, we have been able to come up with a satisfactory solution in Section 2.2. The asymptotics of the obtained fit can fully be elucidated under both separate and simultaneous monotonicity and concavity constraints, but its implementation requires the more complex second-order cone programming. It is also possible to incorporate multiple simultaneous shape constraints into the estimation procedure by using any higher-order polynomial spline referring to the work of Papp and Alizadeh (2013). However, one can only use the truncated power function basis for the implementation of the estimators based on cubic or higher-order splines.

2.1 Quadratic splines and linear programming

Denote a partition of $[0, 1]$ by $0 = t_0 < t_1 < \cdots < t_{k_n} = 1$. Let $N = k_n + p$ and $\pi(x) = (\pi_1(x), \ldots, \pi_N(x))^T$ be the vector of normalized B-splines of order $p + 1$ based on the knot mesh $\{t_j\}$ (see, *e.g.*, Schumaker (2007)). To characterize monotonicity as linear constraints at the knots, we choose to use quadratic splines that correspond to $p = 2$. We then estimate the frontier function $\varphi(x)$ by $\hat{\varphi}_n(x) = \pi(x)^T \hat{\alpha}$, where $\hat{\alpha}$ minimizes

$$\int_0^1 \pi(x)^T \alpha \, dx = \sum_{j=1}^N \alpha_j \int_0^1 \pi_j(x) \, dx \tag{2}$$

over $\alpha \in \mathbb{R}^N$ subject to envelopment and monotonicity constraints, or equivalently,

$$\pi(x_i)^T \alpha \geq y_i \quad i = 1, \ldots, n, \quad \text{and} \quad \pi'(t_j)^T \alpha \geq 0 \quad j = 0, 1, \ldots, k_n, \tag{3}$$

with π' being the continuous, piecewise linear derivative of π. It is easily seen that $\hat{\alpha}$ is identical to the maximum likelihood estimator of the parameter α in the special case where data are independent and have a uniform density on the region $\Psi = \{(x, y) \, | \, 0 \leq x \leq 1, \ 0 \leq y \leq \varphi(x; \alpha)\}$, where $\varphi(x; \alpha) = \pi(x)^T \alpha$.

From a computational point of view, minimizing (2) under (3) is an *inequality form* linear program as the objective and constraint functions are all affine and the problem has no equality constraints. Note that the monotonicity adds $k_n + 1$ linear constraints to n of them already in use. As the number of knots k_n is usually small, the added computational burden is negligible. By introducing slack variables $s = (s_1, \ldots, s_{n+k_n+1})^T$ for the inequalities and expressing the variable α as the difference of two nonnegative variables α^+ and α^-, this minimization problem can be solved by applying any linear programming algorithm to

$$
\begin{aligned}
\text{minimize} \quad & \int_0^1 \pi(x)^T (\alpha^+ - \alpha^-) dx \\
\text{subject to} \quad & \pi(x_i)^T (\alpha^+ - \alpha^-) = y_i + s_i \quad i = 1, \ldots, n, \\
& \pi'(t_j)^T (\alpha^+ - \alpha^-) = s_{n+1+j} \quad j = 0, \ldots, k_n, \\
& \alpha^+ \geq 0, \ \alpha^- \geq 0, \ s \geq 0,
\end{aligned}
$$

which is a linear program in *standard form*, with variables α^+, α^-, and s (see *e.g.* Boyd and Vandenberghe (2004)). The inequalities here have to be understood componentwise.

As is typical in nonparametric estimation, the selection of knots is critical to the performance of the spline smoother $\hat{\varphi}_n$. It is usual to pick out a set of knots equally spaced in percentile ranks by taking $t_j = x_{[jn/k_n]}$, the j/k_nth quantile of the values of x_i for $j = 1, \ldots, k_n - 1$ (see, *e.g.*, He and Shi (1998)). However, considering the special connection of our estimator

$\hat{\varphi}_n$ with the conventional FDH frontier estimator, one can propose an easier way of choosing the knot mesh. The monotone envelopment FDH estimator of φ, defined explicitly as

$$\varphi_n(x) = \max\{y_i,\, i : x_i \leq x\},$$

represents the lowest nondecreasing function that covers the data points $(x_1, y_1), \ldots, (x_n, y_n)$. Then, a monotone function envelopes all the (x_i, y_i)'s if and only if it envelopes the extreme FDH points (x_i, y_i) such that $y_i = \varphi_n(x_i)$. Therefore, the spline smoother $\hat{\varphi}_n$ is identical to the smallest monotone majorant of the FDH function φ_n in the space of quadratic B-splines, and hence the envelopment constraint in (3) reduces to

$$\pi(\mathcal{X}_i)^T \alpha \geq \mathcal{Y}_i \quad i = 1, \ldots, \mathcal{N},$$

where $(\mathcal{X}_1, \mathcal{Y}_1), \ldots, (\mathcal{X}_\mathcal{N}, \mathcal{Y}_\mathcal{N})$ are the observations (x_i, y_i) lying on the FDH boundary. This might suggest using the set of knots $\{t_j = \mathcal{X}_{[j\mathcal{N}/k_n]},\ j = 1, \ldots, k_n - 1\}$ among the FDH points from the intuition that the X-locations of FDH points are more appropriate as knots than those of other usual observations. On the other hand, since the number of knots k_n determines the complexity of the spline approximation, we may view the choice of k_n as model selection through the minimization of the following two information criteria:

$$
\begin{aligned}
AIC(k) &= \log\left(\sum_{i=1}^{n} |y_i - \hat{\varphi}_n(x_i)|\right) + 2(k+2)/n, & (4) \\
BIC(k) &= \log\left(\sum_{i=1}^{n} |y_i - \hat{\varphi}_n(x_i)|\right) + \log n \cdot (k+2)/n. & (5)
\end{aligned}
$$

The first one is similar to the famous Akaike information criterion (Akaike, 1973) and the second one to the Bayesian information criterion (Schwartz, 1978). Both criteria seem to work reasonably well in our simulations and real data analysis. The asymptotic theory in the next section shows that the optimal number of knots is in the order of $n^{1/(3\gamma+1)}$, where $\gamma > 0$ stands for the sharpness degree, or equivalently, the quantity $(\gamma - 1)$ describes the rate at which the joint density f of the data tends to zero (in case $\gamma > 1$) or to infinity (in case $\gamma < 1$) at the boundary. When the density has sudden jumps at the boundary (in case $\gamma = 1$), the optimal number of knots is in the order of $n^{1/4}$. Given that the selection of smoothing parameters is typically a hard problem in nonparametric boundary regression [see, *e.g.*, Hall *et al.* (1998), Hall and Park (2004) and Daouia *et al.* (2010)], our method benefits from an important advantage of having a simple and effective smoothing parameter selector.

When the true frontier function φ is strictly increasing, the monotonicity of the estimate $\hat{\varphi}_n$ is obtained "free of charge", at least in the asymptotic sense.

Proposition 1. *Let $\tilde{\varphi}_n(x) = \pi(x)^T \tilde{\alpha}$ be the unconstrained B-spline estimator, where $\tilde{\alpha} \in \mathbb{R}^N$ minimizes (2) only subject to the data envelopment constraints in (3). Suppose φ has a continuous and strictly positive derivative φ' on $[0,1]$ and $\max_{1 \leq j \leq k_n} |\tilde{\varphi}'_n(t_j) - \varphi'(t_j)| = o(1)$ almost surely. Then*

$$\mathbb{P}[\tilde{\varphi}_n = \hat{\varphi}_n, \; n \to \infty] = 1.$$

Thus the asymptotic properties of $\tilde{\varphi}_n$ hold automatically for $\hat{\varphi}_n$, and we get the monotonicity free of charge. The basic argument is to show that the continuous piecewise linear derivative $\tilde{\varphi}'_n$ of $\tilde{\varphi}_n$ is eventually strictly positive with probability one. The strong uniform convergence of $\tilde{\varphi}_n$ and its derivative is proved in the next section. The asymptotic rates of uniform convergence are also provided there.

When the monotone boundary curve is also known or required to be concave, the linear programming problem of (2) and (3) can easily be expanded to include the additional concavity constraints

$$\pi''(t_j^*)^T \alpha \leq 0 \quad j = 1, \ldots, k_n, \tag{6}$$

that are linear, where π'' denotes the second derivative of π and t_j^* stands for the midpoint of $(t_{j-1}, t_j]$. The second derivative of a quadratic spline exists on each inter-knot interval and is constant. We then estimate φ by $\hat{\varphi}_n^\star(x) = \pi(x)^T \hat{\alpha}^\star$, where $\hat{\alpha}^\star \in \mathbb{R}^N$ minimizes (2) subject to (3) and (6).

Arguably, the best known estimator for preserving both concavity and monotonicity is the DEA frontier. This piecewise linear estimator being, by construction, the smallest concave nondecreasing curve covering all the (x_i, y_i)'s, it is necessarily enveloped by the constrained smoother $\hat{\varphi}_n^\star$, and the envelopment constraints in the linear program are equivalent to

$$\pi(\mathcal{X}_i^*)^T \alpha \geq \mathcal{Y}_i^* \quad i = 1, \ldots, \mathcal{M},$$

where $(\mathcal{X}_1^*, \mathcal{Y}_1^*), \ldots, (\mathcal{X}_{\mathcal{M}}^*, \mathcal{Y}_{\mathcal{M}}^*)$ denote the observations (x_i, y_i) lying on the DEA frontier.

Regarding the choice of knots for computing the optimal concave spline $\hat{\varphi}_n^\star$, an easy option for it is just applying the same scheme as for $\hat{\varphi}_n$ by replacing the FDH points $(\mathcal{X}_i, \mathcal{Y}_i)$ with the DEA points $(\mathcal{X}_i^*, \mathcal{Y}_i^*)$ in the selection criteria (4) and (5). Typically, the number of DEA points is very small compared to the sample size. As such, our experience with real and simulated data indicates that the strategy of just using all the DEA points as knots is also working quite well for datasets of modest size.

The constrained fit $\hat{\varphi}_n^\star$ is similar to the unconstrained estimate $\tilde{\varphi}_n$ in terms of computational complexity and computing expedience using linear program. Asymptotically, both smoothers coincide with probability one under the conditions of the following proposition.

Proposition 2. *Suppose the conditions of Proposition 1 hold. If φ has a continuous and strictly negative second derivative φ'' on $[0,1]$ and $\max_{1 \le j \le k_n} |\tilde{\varphi}_n''(t_j^*) - \varphi''(t_j^*)| = o(1)$ almost surely, then $\mathbb{P}[\tilde{\varphi}_n = \hat{\varphi}_n^\star, \, n \to \infty] = 1$.*

Unfortunately, posing the question of strong uniform convergence of $\tilde{\varphi}_n''$ on the subintervals (t_{j-1}, t_j) involves some mathematical difficulties that we have not yet succeeded in overcoming. We shall need higher-order splines to obtain the uniform convergence of the second derivative $\tilde{\varphi}_n''$ as established below in Theorem 1.

All of the methods described above, including computation of $\tilde{\varphi}_n$, $\hat{\varphi}_n$ and $\hat{\varphi}_n^\star$ via linear programming and knot selection, have been implemented for the R package *npbr* (Daouia, Laurent and Noh (2013)). Next, we propose an entirely satisfactory cubic spline based approach that can handle separate as well as simultaneous monotonicity and concavity constraints.

2.2 Cubic splines and second-order conic programming

Denote a partition of $[0,1]$ by $0 = t_0 < t_1 < \cdots < t_{k_n} = 1$. Let $N = k_n + p$ and $\pi(x) = (\pi_0(x), \pi_1(x), \ldots, \pi_{N-1}(x))^T = (1, x, \ldots, x^p, (x-t_1)_+^p, \ldots, (x-t_{k_n-1})_+^p)^T$ be a vector of power basis based on the knot mesh $\{t_j\}$ with $a_+ = \max\{0, a\}$. We choose here to use cubic splines that correspond to $p = 3$. We then estimate $\varphi(x)$ by $\tilde{\varphi}_n(x) = \pi(x)^T \tilde{\alpha}$, where $\tilde{\alpha}$ minimizes

$$\int_0^1 \pi(x)^T \alpha \, dx = \sum_{j=0}^{N-1} \alpha_j \int_0^1 \pi_j(x) \, dx \qquad (7)$$

over $\alpha = (\alpha_0, \alpha_1, \ldots, \alpha_{k_n+p-1})^T \in \mathbb{R}^N$ subject to the envelopment constraint

$$\pi(x_i)^T \alpha \ge y_i, \quad i = 1, \ldots, n.$$

This defines the unconstrained cubic spline estimator of the frontier function. Given that the second derivative of cubic splines is a linear spline, the concavity constraint can be characterized as linear constraints at the knots t_j themselves instead of the midpoints t_j^* in the case of quadratic splines, that is,

$$\pi''(t_j)^T \alpha \le 0, \quad j = 0, 1, \ldots, k_n.$$

In contrast, since the first derivative of cubic splines is a quadratic spline, the monotonicity constraint can no longer be formulated into linear constraints at the knots. Yet, it is possible to come up with an alternative appealing representation of monotonicity as standard second-order cone constraints thanks to the following proposition.

Proposition 3 (Karlin and Studden, 1966). *Let $p(x) = p_0 + p_1 x + p_2 x^2$ be a quadratic polynomial. Then $p(x) \geq 0$ for all $x \in [0,1]$ if and only if there exists $y_0 \geq 0$ such that $(p_0 + p_2 + y_0, p_0 - p_2 - y_0, p_1 - y_0)^\top \in \mathcal{Q}_3$, where $\mathcal{Q}_{k+1} = \{(z_0, \ldots, z_k) : z_0 \geq \|(z_1, \ldots, z_k)^\top\|_2\}$ is the $(k+1)-$dimensional second order cone, with $\|\cdot\|_2$ being the L_2 norm.*

This well-known characterization of nonnegative quadratic polynomials easily extends to a characterization of monotone cubic splines. Indeed, suppose that we have a cubic spline $f(x) = \sum_{j=0}^{3} \alpha_j x^j + \sum_{j=4}^{k_n+2} \alpha_j (x - t_{j-3})_+^3$. Then the monotonicity constraint means that for all $j = 1, \ldots, k_n$,

$$f'((t_j - t_{j-1})z + t_{j-1}) \geq 0 \quad \text{for all } z \in [0,1].$$

This inequality can be re-expressed as

$$\alpha_1 + 2t_{j-1}\alpha_2 + 3t_{j-1}^2\alpha_3 + \sum_{l=1}^{j-1} 3\alpha_{l+3}(t_{j-1} - t_l)^2$$

$$+ \left\{ 2(t_j - t_{j-1})\alpha_2 + 6(t_j - t_{j-1})t_{j-1}\alpha_3 + \sum_{l=1}^{j-1} 6\alpha_{l+3}(t_j - t_{j-1})(t_{j-1} - t_l) \right\} z$$

$$+ \left\{ 3\alpha_3(t_j - t_{j-1})^2 + \sum_{l=1}^{j-1} 3\alpha_{l+3}(t_j - t_{j-1})^2 \right\} z^2$$

$$= p_{0j} + p_{1j}z + p_{2j}z^2 \geq 0 \quad \text{for all } z \in [0,1], \tag{8}$$

with obvious definitions for p_{0j}, p_{1j} and p_{2j}. When $j = 1$, we define all the summations in (8) to be zero. Let $u = (\alpha^T, (y^0)^T)^T$ where $y^0 = (y_1^0, \ldots, y_{k_n}^0)^T$ and $y_j^0 \geq 0$ for $j = 1, \ldots, k_n$. When $j = 2, \ldots, k_n$, note that $p_{0j} + p_{2j} + y_j^0 = (d_j^T, e_{j,k_n}^T)^T u := c_j^T u$, where

$$d_j = (0, 1, 2t_{j-1}, 6t_{j-1}^2 - 6t_{j-1}t_j + 3t_j^2, 3((t_{j-1} - t_1)^2 + (t_j - t_{j-1})^2), \ldots, 3(t_j - t_{j-1})^2, 0, \cdots, 0)^T \in \mathbb{R}^N$$

and e_{j,k_n} is a standard unit vector of $\mathbb{R}^{k_n}$ with the jth element being 1. Moreover, $p_{0j} - p_{2j} - y_j^0 = (B_{1j}^T, -e_{j,k_n}^T)^T u := A_{1j}^T u$, where

$$B_{1j} = (0, 1, 2t_{j-1}, 6t_{j-1}t_j - 3t_j^2, 3((t_{j-1} - t_1)^2 - (t_j - t_{j-1})^2), \ldots, -3(t_j - t_{j-1})^2, 0, \cdots, 0)^T \in \mathbb{R}^N$$

and $p_{1j} - y_j^0 = (B_{2j}^T, -e_{j,k_n}^T)^T u := A_{2j}^T u$, with

$$B_{2j} = (0, 0, 2(t_j - t_{j-1}), 6(t_j - t_{j-1})t_{j-1}, 6(t_j - t_{j-1})(t_{j-1} - t_1), \ldots, 0, 0, \cdots, 0)^T \in \mathbb{R}^N.$$

Therefore, according to Proposition 3, the monotonicity constraint means that there exist A_{1j}, A_{2j} and $y^0 = (y_1^0, \ldots, y_{k_n}^0)^T$ with $y_j^0 \geq 0$ such that $\|(A_{1j}^T u, A_{2j}^T u)^T\|_2 \leq c_j^T u$ for every $j = 2, \ldots, k_n$ (called second-order cone constraints), where $u = (\alpha^T, (y^0)^T)^T$. It is not hard to verify that the second-order cone constraint holds when $j = 1$. This is the key argument

for the estimation of the unknown parameters α of the constrained nondecreasing cubic spline to be formulated into a second-order cone programming (SOCP) problem.

In summary, cubic spline smoothing under monotonicity and/or concavity constraints requires solving the following typical convex programming problem with respect to $u = (\alpha^T, (y^0)^T)^T$:

$$\text{minimize} \quad \left(\int_0^1 \pi_0(x)\, dx, \ldots, \int_0^1 \pi_{N-1}(x)\, dx, 0_{k_n} \right)^T u \tag{9}$$

$$\text{subject to} \quad \|A_j u\|_2 \leq c_j^T u, \ j = 1, \ldots, k_n, \qquad \text{(monotonicity contraints)}$$

$$(\pi''(t_j)^T, 0_{k_n})u \leq 0, \ j = 0, \ldots, k_n, \quad \text{(concavity constraints)}$$

$$(\pi(x_i)^T, 0_{k_n})u \geq y_i, \ i = 1, \ldots, n, \quad \text{(envelopment constraints)}$$

$$[\, O_{k_n, N}, \ I_{k_n} \,] u \geq 0_{k_n}.$$

Here, $A_j = (A_{1j}, A_{2j})^T$, 0_{k_n} is a zero vector of size k_n, $O_{k_n, N}$ is a $k_n \times N$ zero matrix and I_{k_n} is the identity matrix of dimension k_n. Since both concavity and envelopment constraints are linear ones, and hence are second-order cone constraints, the problem (9) is identical to a standard SOCP problem (see the review article by Alizadeh and Goldfarb (2003)). This optimization model is solvable with minimal running time using available off-the-shelf softwares. We may take any solution to be our estimate. For our numerical simulations and real data analysis, we used CVX, a MATLAB-based free package for specifying and solving convex programs because of its user-friendly nature and efficient implementation (for details, refer to Grant and Boyd (2008, 2013)).

When only the monotonicity constraint is of interest, we estimate the frontier function $\varphi(x)$ by $\check{\varphi}_n(x) = \pi(x)^T \check{\alpha}$, where $\check{\alpha} \in \mathbb{R}^N$ is the solution of the SOCP problem (9) without the concavity constraint. Under the monotonicity and concavity constraints, we estimate $\varphi(x)$ by $\check{\varphi}_n^\star(x) = \pi(x)^T \check{\alpha}^\star$, where $\check{\alpha}^\star$ is the solution of the full optimization problem (9). Next, we show that both restricted estimators $\check{\varphi}_n$ and $\check{\varphi}_n^\star$ inherit the same asymptotic properties as the unrestricted version $\tilde{\varphi}_n$.

Proposition 4. *Let $\tilde{\varphi}_n(x) = \pi(x)^T \tilde{\alpha}$ be the unconstrained cubic spline estimator, where $\tilde{\alpha} \in \mathbb{R}^N$ minimizes (7) only subject to data envelopment. If φ has a continuous and strictly positive derivative φ' on $[0,1]$ with $\sup_{x \in [0,1]} |\tilde{\varphi}_n'(x) - \varphi'(x)| = o(1)$ almost surely, then*

$$\mathbb{P}[\tilde{\varphi}_n = \check{\varphi}_n, \ n \to \infty] = 1.$$

If in addition φ has a continuous and strictly negative second derivative φ'' on $[0,1]$ with $\sup_{x \in [0,1]} |\tilde{\varphi}_n''(x) - \varphi''(x)| = o(1)$ almost surely, then

$$\mathbb{P}[\tilde{\varphi}_n = \check{\varphi}_n^\star, \ n \to \infty] = 1.$$

The next section provides indicative asymptotic rates of uniform convergence for the derivatives $\tilde{\varphi}'_n$ and $\tilde{\varphi}''_n$ of the unconstrained estimate.

In what regards the knot selection process, the same powerful way of regularizing the quadratic spline estimates $\hat{\varphi}_n$ and $\hat{\varphi}^\star_n$, described in Section 2.1, can be applied to the cubic spline versions $\check{\varphi}_n$ and $\check{\varphi}^\star_n$, respectively. The asymptotic theory in the following section shows that the optimal number of knots is in the order of $n^{1/(4\gamma+1)}$ for cubic spline smoothing, and hence a smaller number of knots is typically needed relative to quadratic spline smoothing.

3   Some asymptotic results

Due to the arguments made earlier in Propositions 1 and 4, the asymptotic properties of the unconstrained spline estimate $\tilde{\varphi}_n$ carry over automatically to the monotonic quadratic spline frontier $\hat{\varphi}_n$ and to both constrained cubic spline smoothers $\check{\varphi}_n$ and $\check{\varphi}^\star_n$. As a matter of fact, spline smoothing does not appear to have been considered before even in the literature on unconstrained frontier estimation. In this section we initiate a study of such estimation procedures.

Let $0 = t_0 < t_1 < \cdots < t_{k_n} = 1$ be a knot sequence. We consider splines of general order $(p+1)$. We first note that any spline function of order $(p+1)$ based on the B-spline basis and knot meshes t_j can be re-expressed as $\pi(x)^T \alpha$, where $\pi(x) = (1, x, \ldots, x^p, (x - t_1)^p_+, \ldots, (x - t_{k_n-1})^p_+)^T$, α is a $(k_n + p)$-dimensional vector and $a_+ = \max\{0, a\}$. Thus, the problem is to minimize $\int_0^1 \pi(x)^T \alpha \, dx$ subject to $y_i \leq \pi(x_i)^T \alpha$ for all $1 \leq i \leq n$.

Let $q_j(x) = x^j - (j+1)^{-1}$ for $1 \leq j \leq p$ and $q_j(x) = (x - t_{j-p})^p_+ - (p+1)^{-1}(1 - t_{j-p})^{p+1}$ for $p+1 \leq j \leq p + k_n - 1$. The unconstrained spline estimator is then $\tilde{\varphi}_n(x) = \pi(x)^T \hat{\alpha}$, where $(\hat{\alpha}_j : 1 \leq j \leq p + k_n - 1)$ minimizes $\max_{1 \leq i \leq n}[y_i - \sum_{j=1}^{p+k_n-1} \alpha_j q_j(x)]$ and

$$\hat{\alpha}_0 = \max_{1 \leq i \leq n} \left[y_i - \sum_{j=1}^{p} \hat{\alpha}_j x_i^j - \sum_{k=1}^{k_n-1} \hat{\alpha}_{p+k}(x_i - t_k)^p_+ \right].$$

Below, we demonstrate the uniform rates of convergence of $\tilde{\varphi}_n$ and its derivatives, which is also of independent interest. We consider the general setting where the density function f of the data (x_i, y_i) may have sudden jumps at its support boundary, decay to zero or rise up to infinity at a speed of power $\gamma - 1$ ($\gamma > 0$) of the distance from the boundary. More specifically, we assume

(A1) $f(x, y) = 0$ for all $y > \varphi(x)$ and $f(x, y) = \gamma[\varphi(x) - y]^{\gamma-1}\mu(x) + o((\varphi(x) - y)^{\gamma-1})$ as $y \uparrow \varphi(x)$ for some $\gamma > 0$, where the function μ is bounded away from zero on $[0, 1]$;

(A2) φ has a bounded $(p+1)$th order derivative on $[0, 1]$;

(A3) $\max_{1 \le j \le k_n}(t_j - t_{j-1})/\min_{1 \le j \le k_n}(t_j - t_{j-1})$ is bounded.

Condition (A1) has been considered in Härdle *et al.* (1995), Hall *et al.* (1998), Gijbels and Peng (2000), Hwang *et al.* (2002) and Daouia *et al.* (2010), to name a few. Note that the case $\gamma \le 1$ corresponds to sharp or fault-type boundaries. When $\gamma > 1$, the density decays to zero smoothly as it approaches the support frontier. The smoothness of the frontier function φ is given in (A2). A similar assumption was used in the usual and more-discussed problems of nonparametric central and/or quantile regression estimation (see, *e.g.*, He and Shi 1998). Condition (A3) is standard in spline smoothing, it can also be found in earlier work by He and Shi (1994). For simplicity, we use $a_n \sim b_n$ to mean that a_n/b_n and b_n/a_n are bounded.

Theorem 1. *Assume that the conditions (A1)–(A3) hold. If $k_n \sim (n/\log n)^{1/[(p+1)\gamma+1]}$, then with probability one*

$$\sup_{x \in [0,1]} |\tilde{\varphi}_n^{(m)}(x) - \varphi^{(m)}(x)| = O\left((n^{-1}\log n)^{(p-m)/[(p+1)\gamma+1]}\right), \quad 0 \le m \le p-1.$$

As a direct consequence of Theorem 1, we get indicative asymptotic rates of global convergence of $\tilde{\varphi}_n$ and its derivative $\tilde{\varphi}_n'$:

$$\sup_{x \in [0,1]} |\tilde{\varphi}_n(x) - \varphi(x)| = O\left((n^{-1}\log n)^{p/[(p+1)\gamma+1]}\right);$$

$$\sup_{x \in [0,1]} |\tilde{\varphi}_n'(x) - \varphi'(x)| = O\left((n^{-1}\log n)^{(p-1)/[(p+1)\gamma+1]}\right).$$

The obtained rates depend on both the sharpness degree γ and the smoothness order p. The smaller γ, the faster the attainable uniform convergence rates are.

Remark 1. In the standard mean and/or median regression, Stone (1982) and He and Shi (1998) established that the optimal rates of uniform convergence are $(n^{-1}\log n)^{p/(2p+1)}$ for the regression curve estimate ($m = 0$) and $(n^{-1}\log n)^{(p-1)/(2p+1)}$ for its derivative ($m = 1$) when the number of knots $k_n \sim (n/\log n)^{1/(2p+1)}$. In this case, the proposed boundary smoothing method attains better convergence rates than the classical central regression if and only if $\gamma < 2p/(p+1)$. This is what happens in the irregular setting $\gamma \le 1$ for all $p \ge 2$.

In regions where the boundary is strictly increasing, we obtain rates of convergence of the monotone quadratic and cubic spline estimates $\hat{\varphi}_n$ and $\check{\varphi}_n$ as well, as can easily be seen from Propositions 1 and 4, respectively.

Corollary 1. *Suppose that the boundary function φ has a continuous and strictly positive derivative φ' on $[0,1]$. If (A1)-(A3) hold and $k_n \sim (n/\log n)^{1/[(p+1)\gamma+1]}$ with $p = 2$ for $\hat{\varphi}_n$*

and $p = 3$ for $\check{\varphi}_n$, then we have with probability one

$$\sup_{x \in [0,1]} |\hat{\varphi}_n(x) - \varphi(x)| = O\left((n^{-1} \log n)^{2/(3\gamma+1)}\right);$$

$$\sup_{x \in [0,1]} |\hat{\varphi}'_n(x) - \varphi'(x)| = O\left((n^{-1} \log n)^{1/(3\gamma+1)}\right),$$

$$\sup_{x \in [0,1]} |\check{\varphi}_n(x) - \varphi(x)| = O\left((n^{-1} \log n)^{3/(4\gamma+1)}\right);$$

$$\sup_{x \in [0,1]} |\check{\varphi}'_n(x) - \varphi'(x)| = O\left((n^{-1} \log n)^{2/(4\gamma+1)}\right).$$

Hence, the higher-order spline $\check{\varphi}_n$ is more appealing than $\hat{\varphi}_n$ for both smoothness and speed of convergence.

We also provide the uniform convergence of $\tilde{\varphi}''_n$ on the unit interval $[0, 1]$, which enables us to get the concavity of the cubic spline $\check{\varphi}_n^\star$ free of charge. According to Theorem 1, if the conditions (A1)-(A3) hold and $k_n \sim (n/\log n)^{1/[(p+1)\gamma+1]}$ with $p = 3$, then

$$\sup_{x \in [0,1]} |\tilde{\varphi}''_n(x) - \varphi''(x)| = O\left((n^{-1} \log n)^{1/(4\gamma+1)}\right)$$

with probability one. By applying Proposition 4 in conjunction with this result, we obtain indicative rates of convergence of the constrained smoother $\check{\varphi}_n^\star$ and its derivatives $\check{\varphi}_n^{\star'}$ and $\check{\varphi}_n^{\star''}$ in regions where the frontier is strictly increasing and concave.

Corollary 2. *Suppose that the boundary function φ has a strictly positive derivative φ' and a continuous and strictly negative second derivative φ'' on $[0, 1]$. If the conditions (A1)-(A3) hold and $k_n \sim (n/\log n)^{1/[(p+1)\gamma+1]}$ with $p = 3$, we have with probability one*

$$\sup_{x \in [0,1]} |\check{\varphi}_n^\star(x) - \varphi(x)| = O\left((n^{-1} \log n)^{3/(4\gamma+1)}\right),$$

$$\sup_{x \in [0,1]} |\check{\varphi}_n^{\star'}(x) - \varphi'(x)| = O\left((n^{-1} \log n)^{2/(4\gamma+1)}\right),$$

$$\sup_{x \in [0,1]} |\check{\varphi}_n^{\star''}(x) - \varphi''(x)| = O\left((n^{-1} \log n)^{1/(4\gamma+1)}\right).$$

4 Monte Carlo evidence

Some numerical evidence is given in this section to demonstrate the superiority of the proposed spline smoothers $\hat{\varphi}_n$, $\check{\varphi}_n$, $\hat{\varphi}_n^\star$ and $\check{\varphi}_n^\star$ over the best known constrained and unconstrained frontier estimators based on data envelopment ideas. Those were the popular linearized FDH (LFDH) and DEA estimators described in Section 1, and the modern local-polynomial smoothing estimator of Hall, Park and Stern (1998). Specifically, the local linear frontier

estimator is defined by

$$\hat{\varphi}_{n,LL}(x) \;=\; \min\Big\{ z : \text{there exists } \theta_1 \text{ such that } y_i \le z + \theta_1(x_i - x)$$
$$\text{for all } i \text{ such that } x_i \in (x - h, x + h)\Big\}.$$

Hall and Park (2004) proposed a bootstrap procedure for selecting the bandwidth h in $\hat{\varphi}_{n,LL}$.

To evaluate finite-sample performance of the constrained spline smoothed estimators in comparison with the various frontier estimates described above, we have undertaken some simulation experiments. The experiments all employ the model $y_i = \varphi(x_i)\,v_i$, where x_i is uniform on $[0,1]$ and v_i, independent of x_i, is Beta(β, β) with values of $\beta = 0.5, 1$ and 3 (corresponding, respectively, to a joint density of the (x_i, y_i)'s tending to infinity, having a jump or converging to zero as it approaches the frontier points). The frontier function φ is either linear $\varphi_a(x) = x$, concave $\varphi_b(x) = x^{1/2}$, or $\varphi_c(x) = \exp(-5 + 10x)/(1 + \exp(-5 + 10x))$.

All the experiments were performed over $N = 200$ independent samples of size $n = 25$, 50, 100 and 200. In Tables 1, 2 and 3 we report the simulation results devoted to accuracy of the seven estimation methods: LFDH, DEA, QS (quadratic spline, $\hat{\varphi}_n$), CS (cubic spline, $\check{\varphi}_n$), LL (local linear), QS-C (concave quadratic spline, $\hat{\varphi}_n^{\star}$) and CS-C (concave cubic spline, $\check{\varphi}_n^{\star}$). To assess the performance of each method, we consider the empirical mean integrated squared error (MISE), the empirical integrated squared bias (IBIAS2) and the empirical integrated variance (IVAR), which are given by

$$\text{MISE} = \frac{1}{N}\sum_{j=1}^{N}\text{ISE}(\hat{\varphi}^{(j)}) := \frac{1}{N}\sum_{j=1}^{N}\left[\frac{1}{I}\sum_{i=0}^{I}\left(\hat{\varphi}^{(j)}(z_i) - \varphi(z_i)\right)^2\right] \tag{10}$$
$$= \frac{1}{I}\sum_{i=0}^{I}\left(\varphi(z_i) - \bar{\hat{\varphi}}(z_i)\right)^2 + \frac{1}{I}\sum_{i=0}^{I}\left[\frac{1}{N}\sum_{j=1}^{N}(\hat{\varphi}^{(j)}(z_i) - \bar{\hat{\varphi}}(z_i))^2\right]$$
$$\equiv \text{IBIAS2} + \text{IVAR},$$

where $\{z_i, i = 0, \dots, I\}$ is an equispaced grid with width $1/I$ over $[0,1]$ with $I = 1000$, $\hat{\varphi}^{(j)}(\cdot)$ is the estimated frontier function from the j-th data sample and $\bar{\hat{\varphi}}(z_i) = N^{-1}\sum_{j=1}^{N}\hat{\varphi}^{(j)}(z_i)$. To guarantee a fair comparison among the different methods, we used the smoothing parameter which minimizes the MISE for the spline estimators (QS and CS) and the local linear estimator (LL). Regarding the concave spline estimators (QS-C and CS-C), we just used all the DEA points as knots for simplicity as explained earlier in Section 2.

Additionally, to see how our automatic selection procedures for k perform in practice, we compared the results when the number of knots is selected by (4) and (5) for the estimators $\hat{\varphi}_n$ and $\check{\varphi}_n$ with the resulting local linear frontier estimator when the optimal bandwidth is chosen by the bootstrap procedure proposed in Hall and Park (2004) [LL-B]. For the sake

of conciseness, we only present the results obtained from the criterion (4) [QS-A and CS-A]. The results from (5) were qualitatively similar to those from (4), so they are omitted. Actually, to initiate Hall and Park (2004)'s bootstrap procedure, we need to set a pilot bandwidth, which we have found to be quite critical to the quality of their procedure. To see how the local linear frontier estimator performs empirically at the best, we used the bandwidth which minimizes the MISE as the pilot bandwidth. Two typical realizations of the experiment, with $\varphi \in \{\varphi_b, \varphi_c\}$, $\beta = 0.5$ and $n = 50$, are shown in Figures 2 and 3.

Overall, the spline-based estimators (QS, CS, QS-A, CS-A, QS-C and CS-C) show better performance than all the other estimators regardless of the boundary type (which depends on β) and the sample size. It is clear that the spline-based estimators enjoy the benefit of smooth approximation in reducing the bias when the true function is smooth as shown in Figures 2 and 3. Moreover, both selection criteria of the number of knots seem to work quite well in practice. It is remarkable that our splined-based estimators (QS-A and CS-A) with empirically chosen knots are performing better than the local linear estimator with the theoretically MISE-optimal bandwidth.

When the true frontier function is concave and monotone ($\varphi = \varphi_a$ or φ_b), we observe that the DEA and the concave spline estimators (QS-C and CS-C) have lower IVARs compared to the other estimators. The reason is that they enjoy both monotonicity and concavity properties, reducing thus the unnecessary sampling variability. Moreover, the concave spline estimators have the added advantage over the DEA estimator of reducing the bias thanks to their modeling flexibility and function approximation power as illustrated in Figure 2.

When the frontier function φ is simply monotone but not concave, the local linear estimator (LL) seems to be a useful alternative to the LFDH estimator if the bandwidth is judiciously chosen. However, the LL frontier lacks of smoothness and has no guarantee of being monotone even if the true frontier is so. Accordingly, following the curvature of the monotone frontier φ, its LL estimator is likely to exhibit substantial bias when the number of data points is not large enough, especially at the sample boundaries, as shown in the left panel of Figure 4. A simple way to remedy to this drawback is by imposing the extra condition $\theta_1 \geq 0$ in the definition of $\hat{\varphi}_{n,LL}(x)$ to get

$$\hat{\varphi}_{n,LL2}(x) = \min\Big\{z : \text{there exists } \theta_1 \geq 0 \text{ such that } y_i \leq z + \theta_1(x_i - x)$$
$$\text{for all } i \text{ such that } x_i \in (x - h, x + h)\Big\}.$$

This version reduces the vexing border defect of the LL estimator as illustrated in the right panel of Figure 4. We actually utilized the improved version $\hat{\varphi}_{n,LL2}(x)$ in all our simulations instead of $\hat{\varphi}_{n,LL}(x)$. Yet, it may be seen from Figure 3 and Table 3 that our spline-based estimators are clearly superior to both the $\hat{\varphi}_{n,LL2}(x)$ estimator (computed with

the theoretically MISE-optimal bandwidth) and the LFDH estimator.

5   Data examples

In this section, we illustrate the utility of the proposed spline-based estimators for the three motivating applications described in the introduction. First, we apply our method to the dataset of 254 observations about the reliability of nuclear reactors. Here, it is important to know both lower and upper limits of fracture toughness of each material as a function of temperature. This translates into estimating both optimal support boundaries. Although our focus in the sections above was only on the estimation of the upper support extremity, similar considerations evidently apply to the estimation of the lower boundary. It may be seen from Figure 5, which shows various estimates of the upper and lower frontier functions, that the spline-based estimates (QS-A and CS-A) suggest better capability of fitting edge data. It may also be noted that the lower frontier estimator via CS-A exhibits, as is to be expected, more smoothness and indicates a convex and monotonely increasing shape for the master curve prediction.

Figure 6 shows the efficient econometric frontier estimates which correspond to the production activity of 123 American electric utility companies and 37 European Air Controllers in the left and right panels, respectively. For each dataset, we plot the QS-A, the CS-A and the QS-C estimators. It appears that the obtained QS-C fits provide more appealing results in terms of stability and smoothness (the CS-C fits were very similar to the QS-C estimates, and hence they are not reported here). This is not a surprise as the joint support of data, production set called, is often assumed in the econometric literature to be convex (see, *e.g.*, Gijbels *et al.* (1999) for the electric utility companies and Daouia *et al.* (2008) for the Air Controllers).

6   Conclusion

We proposed a novel approach using polynomial spline fitting for the problem of constrained nonparametric boundary regression. The method allows to handle both single and multiple shape constrained estimation. We mainly considered monotone and/or concave frontier smoothing. Using cubic splines requires solving a convex programming problem with second-order conic constraints to characterize monotonicity, and only linear constraints to represent both envelopment and concavity constraints. The proposed constrained fits are similar to the unconstrained estimates in terms of computational complexity without sacrificing modeling flexibility and function approximation power. They also have the same asymptotic rate of

strong uniform convergence.

Quadratic spline smoothing results in a simpler linearly constrained model, and the restricted fit is shown to inherit the asymptotic rate of uniform convergence of its unrestricted version only under the monotonicity constraint. The key advantage of the quadratic spline fit over the cubic spline estimate is its computational expedience using linear programming. Additionally, the latter can be implemented only with truncated power function basis rather than the more popular B-spline basis, whereas the former can be implemented using both bases. By contrast, the cubic spline smoother is the winner in terms of both smoothness and speed of global convergence. Although both approaches work quite well and either might be used in practice, we have a particular preference for the cubic spline fit as it exhibited slightly better performance than the quadratic spline estimate in our simulation studies.

The quadratic spline smoothing method has been implemented for the R package *npbr* (Daouia *et al.* 2013) and all the MATLAB codes for the cubic spline smoothing procedure are available upon request. We hope that this will encourage others to explore these devices.

Appendix

A.1 Proof of Proposition 1

The key idea goes as in He and Shi (1998, p. 646). Let $\varepsilon = \inf\{\varphi'(x), x \in [0,1]\}$. We have $\varphi'(t_j) \geq \varepsilon > 0$ for each $j = 1, \ldots, k_n$. Then, by the strong uniform convergence of $\tilde{\varphi}'_n$ to φ' at knots, there exists an n_ε such that for all $n > n_\varepsilon$ and all $j = 1, \ldots, k_n$, we have $\tilde{\varphi}'_n(t_j) > \varphi'(t_j) - \varepsilon/2 \geq \varepsilon/2$. Hence, with probability one, we get $\tilde{\varphi}'_n(t_j) > 0$ at all knots for all $n > n_\varepsilon$. The derivative $\tilde{\varphi}'_n$ being piecewise linear, it follows that $\tilde{\varphi}'_n(x) > 0$ at all $x \in [0,1]$. Therefore $\mathbb{P}[\tilde{\varphi}_n = \hat{\varphi}_n, \ \forall n > n_\varepsilon] = 1$.

A.2 Proof of Proposition 2

Let $\eta = \sup\{\varphi''(x), x \in [0,1]\} < 0$. By the uniform convergence of $\tilde{\varphi}''_n$ to φ'' at midpoints, there exists an n_η such that for all $n > n_\eta$ and all $j = 1, \ldots, k_n$, we have $\tilde{\varphi}''_n(t_j^*) < -\eta/2 + \varphi''(t_j^*) \leq \eta/2 < 0$. Because $\tilde{\varphi}''_n$ is piecewise constant, this implies that $\tilde{\varphi}''_n(x) < 0$ at all $x \in (t_{j-1}, t_j)$, for each $j = 1, \ldots, k_n$, and all $n > n_\eta$. Since $\tilde{\varphi}_n$ is also monotone on $[0,1]$ for all $n > n_\varepsilon$, we get $\mathbb{P}[\tilde{\varphi}_n = \hat{\varphi}_n^\star, \ \forall n > n_\eta \vee n_\varepsilon] = 1$.

A.3 Proof of Proposition 4

Let $\varepsilon = \inf\{\varphi'(x), x \in [0,1]\} > 0$. By the uniform convergence of $\tilde{\varphi}'_n$ to φ' over $[0,1]$, with probability one, there exists an n_ε such that for all $n > n_\varepsilon$, we have $\tilde{\varphi}'_n(x) > \varphi'(x) - \varepsilon/2 \geq \varepsilon/2$

for all $x \in [0,1]$. Hence, with probability one, we get $\tilde{\varphi}'_n(x) > 0$ at all $x \in [0,1]$ and for all n large enough. Whence $\mathbb{P}[\tilde{\varphi}_n = \check{\varphi}_n, \, n \to \infty] = 1$.

Let $\eta = \sup\{\varphi''(x), x \in [0,1]\} < 0$. By the strong uniform convergence of $\tilde{\varphi}''_n$ to φ'', there exists an n_η such that for all $n > n_\eta$ and all $x \in [0,1]$, we have $\tilde{\varphi}''_n(x) < -\eta/2 + \varphi''(x) \leq \eta/2 < 0$. Then $\tilde{\varphi}''_n(x) < 0$ at all $x \in [0,1]$ whenever $n > n_\eta$, which implies the concavity of $\tilde{\varphi}_n$ on $[0,1]$, with probability one. Therefore $\mathbb{P}[\tilde{\varphi}_n = \check{\varphi}_n^\star, \, \forall n > n_\eta \vee n_\varepsilon] = 1$.

A.4   Proof of Theorem 1

Let $z_i = \nu_n(y_i - \varphi(x_i))$ and $\delta_n = \max_{1 \leq j \leq k_n}(t_j - t_{j-1})$, where $\nu_n = n^{1/\gamma}(k_n \log n)^{-1/\gamma}$. From (A3) we have $k_n \delta_n \sim 1$. Here and below, $a_n \sim b_n$ means that a_n/b_n and b_n/a_n are bounded. Let $\omega(f, \delta : [a,b]) = \sup_{0 \leq h \leq \delta} \sup_{a \leq x \leq b-h} |f(x+h) - f(x)|$ be a modulus of continuity of f on the interval $[a,b]$. According to an approximation theorem for spline functions (see Theorem 6.20 in Schumaker, 2007, for example), there exists a $(k_n + p)$-dimensional vector α^* such that, for all $m : 0 \leq m \leq p$,

$$\sup_{t_{j-1} \leq x \leq t_j} |\varphi^{(m)}(x) - \alpha^{*\top}\pi^{(m)}(x)| \leq C_0 \delta_n^{p-m} \omega(\varphi^{(p)}, \delta_n : [t_{j-p-1}, t_{j+p}]), \quad 1 \leq j \leq k_n, \quad \text{(A.1)}$$

where C_0 is a positive constant that depends only on p and we set $t_{-p} = \cdots t_{-1} = 0$, $t_{k_n+1} = \cdots = t_{k_n+p} = 1$. We note that π_{p+j}, the $(p+j)$th component of π, is not p times differentiable at $x = t_{j-1}$. In (A.1), $\pi^{(p)}_{p+j}(t_{j-1})$ is understood as the pth right derivative of π at $x = t_{j-1}$. From (A.1) and the condition (A2), we get

$$\sup_{x \in [0,1]} |\varphi^{(m)}(x) - \alpha^{*\top}\pi^{(m)}(x)| \leq C_0' \delta_n^{p+1-m}, \quad 0 \leq m \leq p \quad \text{(A.2)}$$

for some constant $C_0' > 0$.

Define $r_n(x) = \nu_n[\varphi(x) - \pi(x)^T \alpha^*]$ and $\Delta_j = \nu_n(\hat{\alpha}_j - \alpha_j^*)$ for $0 \leq j \leq k_n + p - 1$. For a vector $d = (d_1, \ldots, d_{k_n+p-1})$, let

$$T(d) = \max_{1 \leq i \leq n}\left[z_i - \sum_{j=1}^{p+k_n-1} d_j q_j(x_i) + r_n(x_i)\right].$$

Thus, $\Delta = (\Delta_1, \ldots, \Delta_{k_n+p-1})$ minimizes $T(d)$. We note that

$$\nu_n \sup_{x \in [0,1]} |\tilde{\varphi}_n(x) - \varphi(x)| = \sup_{x \in [0,1]} |\pi(x)^T \Delta - r_n(x)|$$

$$\leq \sum_{j=0}^{p} |\Delta_j| + \sum_{j=1}^{k_n-1}(1-t_j)^p|\Delta_{p+j}| + \sup_{x \in [0,1]} |r_n(x)| \quad \text{(A.3)}$$

$$\leq |\Delta_0| + \sum_{j=1}^{p} |\Delta_j| + c\sum_{j=p+1}^{p+k_n-1}\left(1 - \frac{j-p}{k_n}\right)^p |\Delta_j| + \sup_{x \in [0,1]} |r_n(x)|.$$

19

Here and below, c denotes the generic positive constant that depends only on p. We take $\delta_n \sim (n^{-1}\log n)^{1/((p+1)\gamma+1)}$, so that $\sup_{x\in[0,1]} |r_n(x)| = O(\nu_n \delta_n^{p+1}) = O(1)$ by (A.2).

We first prove

$$W_n \equiv \sum_{j=1}^{p} |\Delta_j| + \sum_{j=p+1}^{p+k_n-1} \left(1 - \frac{j-p}{k_n}\right)^p |\Delta_j| = O(k_n) \tag{A.4}$$

with probability one. Let $\xi_j = (j+1)^{-1/j}$ for $1 \le j \le p$ and $\xi_{p+k} = t_k + (p+1)^{-1/p}(1-t_k)^{1+(1/p)}$ for $1 \le k \le k_n - 1$. Then, $0 = \xi_0 < \xi_1 < \cdots < \xi_{p+k_n-1} < \xi_{p+k_n} = 1$. Write $\xi_{j,1} = \xi_{j-1} + (\xi_j - \xi_{j-1})/3$ and $\xi_{j,2} = \xi_{j-1} + 2(\xi_j - \xi_{j-1})/3$. Let I_j denote the interval $[\xi_{j,1}, \xi_{j,2}]$. Then, there exists a constant $c > 0$ such that

$$(\text{length of } I_j) \ge c, \quad 1 \le j \le p. \tag{A.5}$$

Let $g(t) = t + (p+1)^{-1/p}(1-t)^{1+(1/p)}$. Then, g' is strictly increasing so that $g'(t) \ge g'(0) = 1 - p^{-1}(p+1)^{1-(1/p)}$ for all $t \in [0,1]$ and $g'(0) > 0$ for all $p > 1$. This means

$$\xi_{p+j+1} - \xi_{p+j} = g(t_{j+1}) - g(t_j) \ge g'(0)(t_{j+1} - t_j),$$

so that there exists a constant $c > 0$ such that

$$(\text{length of } I_j) \ge c\delta_n, \quad p+1 \le j \le p+k_n. \tag{A.6}$$

Here, we have used the condition (A3). Arguing as in the proof of Theorem 2.1 of Hall, Park and Stern (1998), there exists a random integer $1 \le J \le p + k_n$ such that $\Delta_j < 0$ for all $j < J$ and $\Delta_j \ge 0$ for all $j \ge J$. We claim that there exists an absolute constant $c_0 > 0$ such that, on the event $J = j$,

$$\sup_{x\in I_j} \sum_{l=1}^{p+k_n-1} \Delta_l q_l(x) \le -c_0 W_n/k_n. \tag{A.7}$$

This implies that, for a sufficiently large $C > 0$,

$$
\begin{aligned}
P(W_n > Ck_n) &\le \sum_{j=1}^{p+k_n} P\left[-\frac{1}{c_0} \sup_{x\in I_j} \sum_{l=1}^{p+k_n-1} \Delta_l q_l(x) > C, J = j \right] \\
&\le \sum_{j=1}^{p+k_n} P\left[T(\Delta) \ge \max_{i:x_i\in I_j} z_i + \frac{2}{3}c_0 C, J = j \right] \\
&\le \sum_{j=1}^{p+k_n} P\left[T(0) \ge \max_{i:x_i\in I_j} z_i + \frac{2}{3}c_0 C, J = j \right] \\
&\le \sum_{j=1}^{p+k_n} P\left(\max_{i:x_i\in I_j} z_i \le -\frac{1}{3}c_0 C \right).
\end{aligned}
\tag{A.8}
$$

The second inequality of (A.8) follows from the facts that $\sup_{x\in[0,1]} |r_n(x)| = O(1)$ and $T(\Delta) \geq \max_{i:x_i\in I_j}[z_i - \sum_{l=1}^{p+k_n-1} \Delta_l q_l(x_i) + r_n(x_i)]$. The fourth inequality holds since $T(0) \leq \sup_{x\in[0,1]} |r_n(x)|$.

The event $\max_{i:x_i\in I_j} z_i \leq -c_0 C/3$ occurs if and only if there is no (x_i, y_i) in the set $A_n \equiv \{(x,y) : x \in I_j, y \in [\varphi(x) - \nu_n^{-1}c_0 C/3, \varphi(x)]\}$. From (A.5) and (A.6) it follows that

$$P[(x_i, y_i) \in A_n] = \int_{A_n} f(x, y)\, dy\, dx \geq c \cdot c_0^\gamma \cdot C^\gamma \frac{\log n}{n}(1 + o(1)) \tag{A.9}$$

for some constant $c > 0$. This implies

$$\sum_{j=1}^{p+k_n} P\left(\max_{i:x_i\in I_j} z_i \leq -\frac{1}{3}c_0 C\right) \leq (p + k_n)n^{-c\cdot C^\gamma} \tag{A.10}$$

for some constant $c > 0$, so that $\sum_{n=1}^\infty P(W_n > Ck_n) < \infty$ for sufficiently large $C > 0$. This proves (A.4).

To prove $|\Delta_0| = O(k_n)$ with probability one, we note that

$$|\Delta_0| \leq \left| \max_{1\leq i\leq n}\left(z_i - \sum_{j=1}^{p+k_n-1} \Delta_j \pi_j(x_i)\right)\right| + \sup_{x\in[0,1]} |r_n(x)|$$
$$\leq -\max_{1\leq i\leq n} z_i + \max\{1, c\}W_n + O(1)$$

for the constant c at (A.3). Since it holds that $-\max_{i\leq i\leq n} z_i = O(k_n^{-1/\gamma})$ with probability one, we get that $|\Delta_0| = O(k_n)$ with probability one, so that

$$\sup_{x\in[0,1]} |\tilde{\varphi}_n(x) - \varphi(x)| = O\left(\nu_n^{-1}k_n + \delta_n^{p+1}\right) = O\left((n^{-1}\log n)^{p/[(p+1)\gamma+1]}\right)$$

with probability one.

Now, for the derivative estimation we note that there exist constants $C_m > 0$ for $1 \leq m \leq p - 1$ such that

$$\nu_n \sup_{x\in[0,1]} |\tilde{\varphi}_n^{(m)}(x) - \varphi^{(m)}(x)| \leq C_m\left[\sum_{j=m}^p |\Delta_j| + k_n^m \sum_{j=p+1}^{p+k_n-1}\left(1 - \frac{j-p}{k_n}\right)^p |\Delta_j|\right]$$
$$+ \sup_{x\in[0,1]} |r_n^{(m)}(x)|$$
$$\leq C_m k_n^m W_n + \sup_{x\in[0,1]} |r_n^{(m)}(x)|.$$

From (A.2) and (A.4), we conclude

$$\sup_{x\in[0,1]} |\tilde{\varphi}_n^{(m)}(x) - \varphi^{(m)}(x)| = O\left(\nu_n^{-1}k_n^{m+1} + \delta_n^{p+1-m}\right) = O\left((n^{-1}\log n)^{(p-m)/[(p+1)\gamma+1]}\right)$$

21

with probability one.

It remains to prove the claim (A.7). Since $q_l(x) < 0$ if $x < \xi_l$ and $q_l(x) \geq 0$ if $x \geq \xi_l$, there exists a constant $c > 0$ such that, for all $x \in I_J = [\xi_{J,1}, \xi_{J,2}]$,

$$q_l(x) \geq c(\xi_{J,1} - \xi_l) \ \text{ if } \ 1 \leq l \leq J - 1,$$
$$q_l(x) \leq -c(\xi_l - \xi_{J,2}) \leq \ \text{ if } \ l \geq \max\{J, p+1\} \ \text{ and } \ \xi_{J,2} \geq t_{l-p},$$
$$q_l(x) = -(1 - t_{l-p})^{p+1}/(p+1) \ \text{ if } \ l \geq \max\{J, p+1\} \ \text{ and } \ \xi_{J,2} < t_{l-p},$$
$$q_l(x) \leq -c(\xi_l - \xi_{J,2}) \ \text{ if } \ J \leq l < \max\{J, p+1\}.$$

We note that, in case $p + 1 \leq l \leq p + k_n - 1$,

$$-\frac{(1 - t_{l-p})^{p+1}}{p+1} \leq -c\left(1 - \frac{l-p}{k_n}\right)^{p+1}$$

for some constant $c > 0$. Define $l(J) = \max\{J, p+1\}$ and for $l(J) \leq l \leq p + k_n - 1$

$$a(J, l) = (\xi_l - \xi_{J,2})I(\xi_{J,2} \geq t_{l-p}) + \left(1 - \frac{l-p}{k_n}\right)^{p+1} I(\xi_{J,2} < t_{l-p}).$$

Since $\Delta_l < 0$ for all $l < J$ and $\Delta_l \geq 0$ for all $j \geq J$, there exists a constant $c > 0$ such that, for all $x \in I_J$,

$$\sum_{l=1}^{p+k_n-1} \Delta_l q_l(x) \leq -c \left[\sum_{l=1}^{J-1}(\xi_{J,1} - \xi_l)|\Delta_l| + \sum_{l=J}^{l(J)-1} (\xi_l - \xi_{J,2})|\Delta_l| + \sum_{l=l(J)}^{p+k_n-1} a(J, l)|\Delta_l| \right].$$

The second sum on the right hand side of the above inequality is set to be zero in case $l(J) = J$, i.e., $J \geq p + 1$. Now, we note that $\xi_{J,1} - \xi_l \geq (\xi_J - \xi_{J-1})/3 \geq ck_n^{-1}$ for all $1 \leq l \leq J - 1$ and $\xi_l - \xi_{J,2} \geq (\xi_J - \xi_{J-1})/3 \geq ck_n^{-1}$ for all $J \leq l \leq p + k_n$, where $c > 0$ is a constant. Furthermore, there exists a constant $c > 0$ such that

$$a(J, l) \geq ck_n^{-1}\left[I(\xi_{J,2} \geq t_{l-p}) + \left(1 - \frac{l-p}{k_n}\right)^p I(\xi_{J,2} < t_{l-p})\right]$$
$$\geq ck_n^{-1}\left(1 - \frac{l-p}{k_n}\right)^p.$$

These entail that, for some constant $c_0 > 0$,

$$\sum_{l=1}^{p+k_n-1} \Delta_l q_l(x) \leq -c_0 k_n^{-1}\left[\sum_{l=1}^{l(J)-1} |\Delta_l| + \sum_{l=l(J)}^{p+k_n-1} \left(1 - \frac{l-p}{k_n}\right)^p |\Delta_l| \right] \leq -c_0 k_n^{-1} W_n$$

for all $x \in I_J$.

22

References

[1] Akaike, H. (1973), Information theory and an extension of the maximum likelihood principle, in *Second International Symposium of Information Theory*, eds. B. N. Petrov and F. Csaki, Budapest: Akademia Kiado, 267–281.

[2] Alizadeh, F. and Goldfarb, D. (2003). Second-order cone programming, *Mathematical Programming Series B*, **95**, 3–51.

[3] Boyd, S. and Vandenberghe, L. (2004). *Convex Optimization*, Cambridge University Press, Cambridge.

[4] Daouia, A., Florens, J.P. and Simar, L. (2008). Functional Convergence of Quantile-type Frontiers with Application to Parametric Approximations, *Journal of Statistical Planning and Inference*, **138** (3), 708–725.

[5] Daouia, A., Florens, J.P. and Simar, L. (2010). Frontier Estimation and Extreme Value Theory, *Bernoulli*, **16**, 1039–1063.

[6] Daouia, A., Laurent, T. and Noh, H. (2013). Nonparametric boundary regression: The *npbr* package, v1.0. Available at http://cran.r-project.org/package=npbr.

[7] de Haan, L. and Resnick, S. (1994). Estimating the home range, *Journal of Applied Probability*, **31**, 700–720.

[8] Dierckx, P. (1993). *Curve and Surface Fitting With Splines*, Oxford, U.K.: Clarendon Press.

[9] Gijbels, I., Mammen, E., Park, B.U. and Simar, L. (1999). On estimation of monotone and concave frontier functions, *Journal of American Statistical Association*, **94**, 220–228.

[10] Gijbels, I. and Peng, L. (2000). Estimation of a support curve via order statistics, *Extremes*, **3**, 251–277.

[11] Girard, S. and Jacob, P. (2003). Extreme values and Haar series estimates of point process boundaries, *Scandinavian Journal of Statistics*, **30** (2), 369–384.

[12] Girard, S. and Jacob, P. (2004), Extreme values and kernel estimates of point processes boundaries. *ESAIM: Probability and Statistics*, **8**, 150–168.

[13] Grant, M. and Boyd, S. (2008), Graph implementations for nonsmooth convex programs, Recent Advances in Learning and Control (a tribute to M. Vidyasagar), V. Blondel, S. Boyd, and H. Kimura, editors, pages 95-110, Lecture Notes in Control and Information Sciences, Springer.

[14] Grant, M. and Boyd, S. (2013), CVX: Matlab software for disciplined convex programming, version 2.0 beta.

[15] Hall, P., Nussbaum, M. and Stern, S.E. (1997). On the estimation of a support curve of indeterminate sharpness, *Journal of Multivariate Analysis*, **62**, 204–232.

[16] Hall, P. and Park, B.U. (2002). New methods for bias correction at endpoints and boundaries, *Annals of Statistics*, **30**, 1460-1479.

[17] Hall, P. and Park, B.U. (2004). Bandwidth choice for local polynomial estimation of smooth boundaries, *Journal of Multivariate Analysis*, **91** (2), 240–261.

[18] Hall, P., Park, B.U. and Stern, S.E. (1998). On polynomial estimators of frontiers and boundaries, *Journal of Multivariate Analysis*, **66**, 71–98.

[19] Härdle, W., Park, B.U. and Tsybakov, A.B. (1995). Estimation of non-sharp support boundaries, *Journal of Multivariate Analysis*, **43**, 205–218.

[20] He, X. and Shi, P. (1994). Convergence rate of B-spline estimators of nonparametric conditional quantile functions, *Nonparametric statistics*, **3**, 299–308.

[21] He, X. and Shi, P. (1998). Monotone B-Spline Smoothing, *Journal of American Statistical Association*, **93**, 643–650.

[22] Hwang, J.H., Park, B.U. and Ryu, W. (2002), Limit theorems for boundary function estimators, *Statistics & Probability Letters*, **59**, 353–360.

[23] Jacob, P. and Suquet, P. (1995). Estimating the edge of a Poisson process by orthogonal series, *Journal of Statistical Planning and Inference*, **46**, 215–234.

[24] Jeong, S.-O. and Park, B.U. (2006). Large sample approximation of the distribution for convex-hull estimators of boundaries, *Scandinavian Journal of Statistics*, **33**, 139–151.

[25] Jeong, S.-O. and Simar, L. (2006). Linearly interpolated FDH efficiency score for non-convex frontiers, *Journal of Multivariate Analysis*, **97**, 2141–2161.

[26] Karlin, S. and Studden, W.J. (1966). *Tchebycheff Systems, with Applications in Analysis and Statistics*. Wiley Interscience Publishers.

[27] Kneip, A., Simar, L. and Wilson, P.W. (2008). Asymptotics and consistent bootstraps for DEA estimators in non-parametric frontier models, *Econometric Theory*, **24**, 1663–1697.

[28] Knight, K. (2001). Limiting distributions of linear programming estimators, *Extremes*, **4** (2), 87–103.

[29] Korostelev, A., Simar, L. and Tsybakov, A.B. (1995). Efficient estimation of monotone boundaries, *Annals of Statistics*, **23**, 476–489.

[30] Korostelev, A. and Tsybakov, A.B. (1993). *Minimax theory of image reconstruction*. Volume 82 of Lecture Notes in Statistics, Springer-verlag, New-York.

[31] Papp, D. and Alizadeh, F. (2013). Shape constrained estimations using nonnegative splines, *Journal of Computational and graphical Statistics*, In press.

[32] Park, B.U., Jeong, S.-O. and Simar, L. (2010). Asymptotic distribution of conical-hull estimators of directional edges, *Annals of Statistics*, **38**, 1320–1340.

[33] Schumaker, L.L. (2007). *Spline Functions: Basic Theory*, 3rd edition, Cambridge University Press.

[34] Schwartz, G. (1978). Estimating the dimension of a model, *Annals of Statistics*, **6**, 461–464.

[35] Stone, C. (1982). Optimal Global Rates of Convergence for Nonparametric Regression, *Annals of Statistics*, **10**, 1040–1053.

[36] Wang, X. and Li, F. (2008). Isotonic Smoothing Spline Regression, *Journal of Computational and Graphical Statistics*, **17** (1), 21–37.
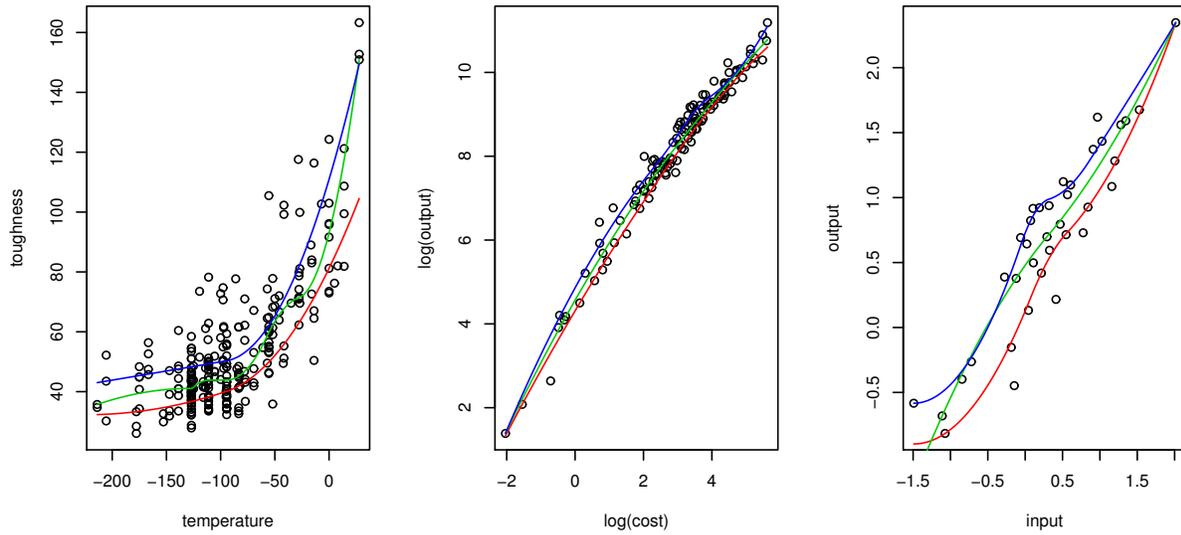
Figure 1: Scatterplots of three real datasets with the quartile curves in each plot. The three regression quantile curves are estimated by the method of He and Shi (1998).
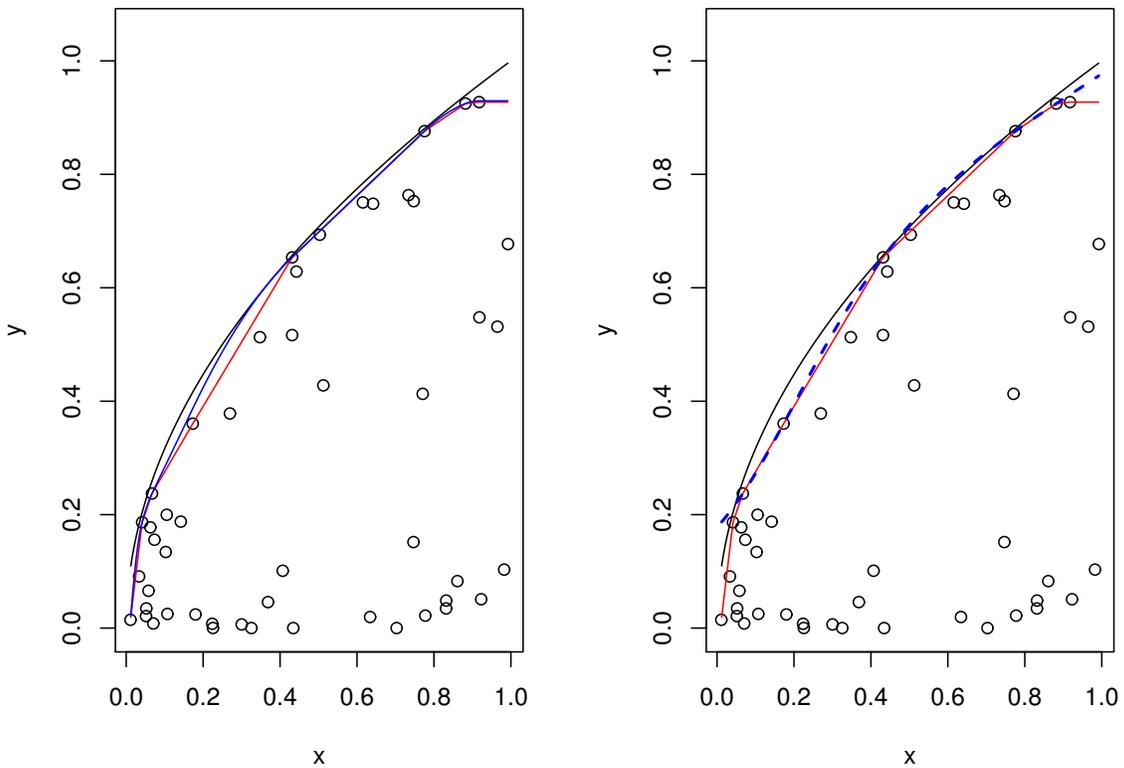
Figure 2: When $n = 50$ and $\beta = 0.5$, the true frontier function (φ_b, black) and its three estimates: DEA(solid red), QS-C (solid blue, left panel) and CS-C (dotted blue, right panel)

Table 1: Comparison when the true frontier is linear ($\varphi(x) = \varphi_a(x)$). All the results are multiplied by 100.

			DEA	QS	CS	LL	QS-C	CS-C	QS-A	CS-A	LL-B
$\beta = 0.5$	$n = 25$	IBIAS2	0.225	0.106	0.094	0.146	0.248	0.122	0.127	0.094	0.255
		IVAR	0.207	0.256	0.146	0.188	0.233	0.173	0.248	0.146	0.256
		IMSE	0.431	0.362	0.241	0.334	0.481	0.294	0.374	0.241	0.512
	$n = 50$	IBIAS2	0.077	0.026	0.022	0.049	0.078	0.037	0.033	0.022	0.078
		IVAR	0.082	0.062	0.049	0.066	0.081	0.064	0.089	0.049	0.081
		IMSE	0.158	0.087	0.071	0.114	0.159	0.101	0.122	0.072	0.159
	$n = 100$	IBIAS2	0.014	0.001	0.001	0.007	0.014	0.004	0.001	0.001	0.014
		IVAR	0.014	0.008	0.004	0.009	0.014	0.008	0.009	0.003	0.014
		IMSE	0.028	0.009	0.005	0.016	0.028	0.011	0.011	0.005	0.028
	$n = 200$	IBIAS2	0.004	0.000	0.000	0.002	0.004	0.001	0.000	0.000	0.004
		IVAR	0.006	0.001	0.001	0.004	0.006	0.003	0.002	0.001	0.006
		IMSE	0.009	0.001	0.001	0.005	0.009	0.004	0.002	0.002	0.009
$\beta = 1$	$n = 25$	IBIAS2	0.589	0.432	0.363	0.446	0.615	0.391	0.523	0.363	0.638
		IVAR	0.254	0.350	0.238	0.252	0.252	0.261	0.372	0.238	0.285
		IMSE	0.843	0.782	0.601	0.699	0.867	0.652	0.894	0.601	0.922
	$n = 50$	IBIAS2	0.217	0.131	0.108	0.149	0.222	0.130	0.184	0.108	0.223
		IVAR	0.099	0.113	0.078	0.080	0.099	0.089	0.161	0.078	0.099
		IMSE	0.317	0.244	0.186	0.230	0.321	0.220	0.345	0.186	0.322
	$n = 100$	IBIAS2	0.120	0.053	0.048	0.082	0.122	0.060	0.084	0.054	0.122
		IVAR	0.055	0.051	0.039	0.042	0.054	0.043	0.077	0.040	0.054
		IMSE	0.175	0.105	0.086	0.124	0.177	0.103	0.161	0.094	0.176
	$n = 200$	IBIAS2	0.031	0.012	0.010	0.022	0.032	0.016	0.022	0.012	0.032
		IVAR	0.015	0.012	0.009	0.012	0.015	0.010	0.026	0.010	0.015
		IMSE	0.047	0.023	0.019	0.035	0.047	0.026	0.048	0.022	0.047
$\beta = 3$	$n = 25$	IBIAS2	2.015	1.834	1.592	1.697	2.083	1.648	2.088	1.594	2.132
		IVAR	0.267	0.387	0.263	0.264	0.260	0.280	0.391	0.261	0.264
		IMSE	2.282	2.221	1.855	1.960	2.343	1.929	2.479	1.855	2.396
	$n = 50$	IBIAS2	1.298	1.162	1.042	1.123	1.353	1.073	1.402	1.048	1.352
		IVAR	0.164	0.200	0.159	0.158	0.160	0.167	0.235	0.159	0.161
		IMSE	1.461	1.362	1.202	1.281	1.513	1.240	1.637	1.207	1.513
	$n = 100$	IBIAS2	0.760	0.661	0.579	0.652	0.789	0.604	0.956	0.595	0.784
		IVAR	0.100	0.130	0.098	0.097	0.095	0.100	0.157	0.098	0.096
		IMSE	0.860	0.791	0.676	0.749	0.884	0.704	1.113	0.694	0.880
	$n = 200$	IBIAS2	0.490	0.418	0.367	0.415	0.504	0.383	0.688	0.383	0.503
		IVAR	0.063	0.086	0.061	0.058	0.062	0.063	0.115	0.063	0.062
		IMSE	0.553	0.504	0.428	0.473	0.566	0.446	0.804	0.446	0.564

Table 2: Comparison when the true frontier is monotone and concave ($\varphi(x) = \varphi_b(x)$). All the results are multiplied by 100.

			DEA	QS	CS	LL	QS-C	CS-C	QS-A	CS-A	LL-B
$\beta = 0.5$	$n = 25$	IBIAS2	0.283	0.112	0.119	0.287	0.190	0.163	0.121	0.119	0.292
		IVAR	0.185	0.257	0.187	0.189	0.197	0.194	0.264	0.187	0.199
		IMSE	0.468	0.368	0.306	0.475	0.387	0.357	0.385	0.306	0.491
	$n = 50$	IBIAS2	0.085	0.016	0.021	0.086	0.052	0.041	0.019	0.021	0.086
		IVAR	0.065	0.077	0.056	0.065	0.067	0.064	0.077	0.056	0.065
		IMSE	0.150	0.094	0.077	0.151	0.119	0.105	0.096	0.077	0.151
	$n = 100$	IBIAS2	0.022	0.003	0.004	0.022	0.012	0.009	0.006	0.004	0.022
		IVAR	0.018	0.018	0.013	0.018	0.017	0.016	0.018	0.013	0.018
		IMSE	0.040	0.021	0.017	0.040	0.029	0.026	0.023	0.017	0.040
	$n = 200$	IBIAS2	0.007	0.001	0.001	0.007	0.004	0.003	0.004	0.002	0.007
		IVAR	0.005	0.005	0.003	0.005	0.005	0.005	0.006	0.004	0.005
		IMSE	0.012	0.005	0.004	0.012	0.009	0.007	0.010	0.006	0.012
$\beta = 1$	$n = 25$	IBIAS2	0.849	0.505	0.498	0.866	0.641	0.573	0.558	0.499	0.889
		IVAR	0.277	0.475	0.302	0.281	0.330	0.328	0.474	0.300	0.302
		IMSE	1.126	0.981	0.800	1.148	0.971	0.901	1.032	0.799	1.191
	$n = 50$	IBIAS2	0.297	0.144	0.143	0.302	0.210	0.186	0.165	0.146	0.301
		IVAR	0.109	0.146	0.117	0.110	0.121	0.112	0.158	0.114	0.109
		IMSE	0.406	0.290	0.260	0.412	0.331	0.298	0.323	0.260	0.410
	$n = 100$	IBIAS2	0.143	0.054	0.063	0.143	0.098	0.088	0.068	0.064	0.143
		IVAR	0.051	0.064	0.053	0.052	0.056	0.055	0.074	0.052	0.052
		IMSE	0.195	0.118	0.117	0.195	0.154	0.143	0.142	0.116	0.195
	$n = 200$	IBIAS2	0.054	0.017	0.020	0.054	0.036	0.030	0.020	0.020	0.054
		IVAR	0.019	0.024	0.017	0.020	0.022	0.020	0.019	0.018	0.019
		IMSE	0.072	0.040	0.038	0.072	0.055	0.050	0.043	0.038	0.072
$\beta = 3$	$n = 25$	IBIAS2	3.096	2.526	2.481	3.140	2.753	2.657	2.765	2.489	3.160
		IVAR	0.288	0.438	0.332	0.289	0.341	0.346	0.417	0.327	0.292
		IMSE	3.384	2.964	2.813	3.429	3.094	3.003	3.182	2.816	3.452
	$n = 50$	IBIAS2	1.987	1.511	1.521	1.999	1.706	1.644	1.714	1.542	2.000
		IVAR	0.198	0.303	0.234	0.198	0.239	0.236	0.311	0.234	0.198
		IMSE	2.184	1.813	1.755	2.197	1.946	1.880	2.025	1.776	2.198
	$n = 100$	IBIAS2	1.287	0.939	0.952	1.295	1.091	1.047	1.165	0.971	1.295
		IVAR	0.104	0.169	0.138	0.104	0.131	0.126	0.178	0.128	0.104
		IMSE	1.391	1.108	1.089	1.400	1.222	1.173	1.342	1.099	1.399
	$n = 200$	IBIAS2	0.813	0.548	0.567	0.815	0.681	0.645	0.776	0.597	0.815
		IVAR	0.075	0.110	0.095	0.075	0.093	0.092	0.138	0.089	0.075
		IMSE	0.888	0.658	0.661	0.890	0.774	0.737	0.914	0.686	0.890

Table 3: Comparison when the true frontier is monotone but not concave ($\varphi(x) = \varphi_c(x)$). All the results are multiplied by 100.

			LFDH	QS	CS	LL	QS-A	CS-A	LL-B
$\beta = 0.5$	$n = 25$	IBIAS2	0.715	0.153	0.207	0.549	0.139	0.185	0.990
		IVAR	0.591	0.637	0.637	0.539	0.526	0.606	0.467
		IMSE	1.306	0.790	0.844	1.087	0.665	0.791	1.457
	$n = 50$	IBIAS2	0.258	0.029	0.035	0.192	0.032	0.034	0.610
		IVAR	0.216	0.154	0.148	0.170	0.180	0.157	0.132
		IMSE	0.474	0.183	0.184	0.362	0.212	0.191	0.743
	$n = 100$	IBIAS2	0.090	0.006	0.005	0.057	0.009	0.004	0.179
		IVAR	0.079	0.042	0.022	0.062	0.053	0.025	0.041
		IMSE	0.169	0.048	0.027	0.119	0.062	0.029	0.220
	$n = 200$	IBIAS2	0.037	0.001	0.001	0.019	0.002	0.000	0.055
		IVAR	0.034	0.011	0.006	0.012	0.013	0.004	0.011
		IMSE	0.071	0.012	0.006	0.031	0.015	0.005	0.065
$\beta = 1$	$n = 25$	IBIAS2	1.477	0.405	0.594	1.064	0.486	0.625	1.324
		IVAR	0.571	0.642	0.732	0.484	0.685	0.653	0.504
		IMSE	2.048	1.047	1.326	1.548	1.171	1.278	1.829
	$n = 50$	IBIAS2	0.788	0.125	0.221	0.545	0.180	0.249	0.726
		IVAR	0.329	0.321	0.305	0.265	0.346	0.344	0.243
		IMSE	1.117	0.446	0.526	0.810	0.526	0.592	0.969
	$n = 100$	IBIAS2	0.392	0.063	0.071	0.233	0.076	0.096	0.309
		IVAR	0.163	0.110	0.115	0.089	0.137	0.106	0.087
		IMSE	0.555	0.173	0.186	0.322	0.213	0.202	0.396
	$n = 200$	IBIAS2	0.169	0.019	0.023	0.087	0.022	0.030	0.111
		IVAR	0.075	0.052	0.032	0.040	0.057	0.035	0.036
		IMSE	0.244	0.070	0.055	0.127	0.079	0.065	0.147
$\beta = 3$	$n = 25$	IBIAS2	3.919	2.023	2.051	3.019	2.407	2.488	3.088
		IVAR	0.438	0.582	0.713	0.375	0.515	0.600	0.437
		IMSE	4.357	2.605	2.765	3.394	2.922	3.088	3.525
	$n = 50$	IBIAS2	2.587	1.054	1.036	2.321	1.398	1.588	2.318
		IVAR	0.270	0.325	0.474	0.214	0.338	0.313	0.215
		IMSE	2.857	1.379	1.510	2.535	1.735	1.901	2.532
	$n = 100$	IBIAS2	1.801	0.594	0.713	1.315	0.944	1.049	1.345
		IVAR	0.200	0.182	0.316	0.138	0.234	0.203	0.145
		IMSE	2.001	0.776	1.029	1.453	1.177	1.253	1.489
	$n = 200$	IBIAS2	1.245	0.319	0.509	0.886	0.629	0.702	0.890
		IVAR	0.134	0.127	0.186	0.089	0.159	0.128	0.092
		IMSE	1.378	0.446	0.695	0.975	0.788	0.829	0.982
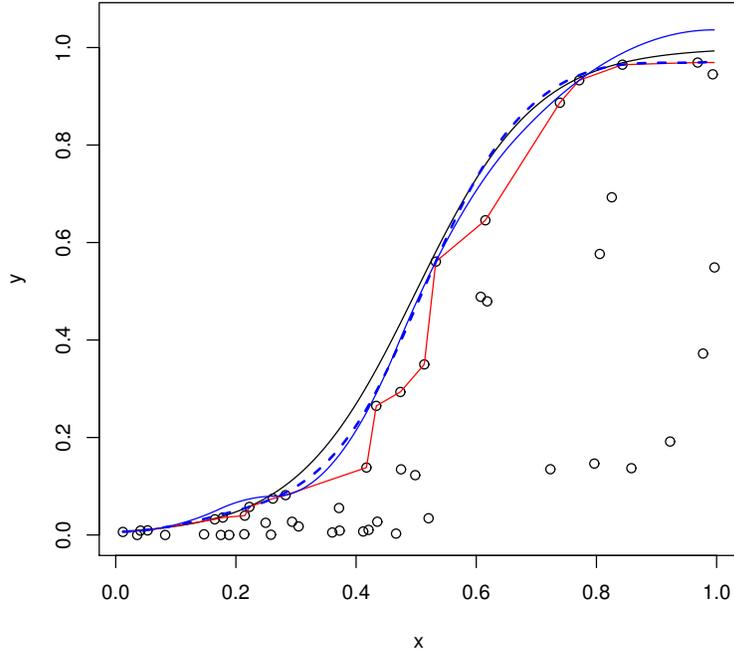
Figure 3: When $n = 50$ and $\beta = 0.5$, the true frontier function (φ_c, black) and its three estimates: LFDH(dotted red), QS-A (solid blue) and CS-A (dotted blue)
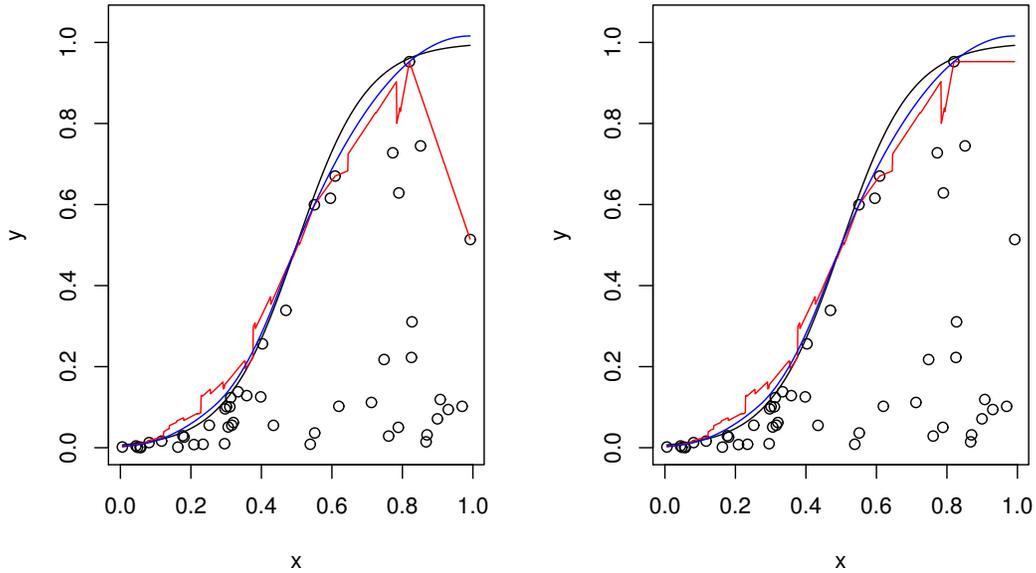
Figure 4: The problem of the local linear frontier estimator (left panel) and the illustration of its improved version (right panel)-LL (red curve), QS-A (blue curve) and the true frontier (black curve)
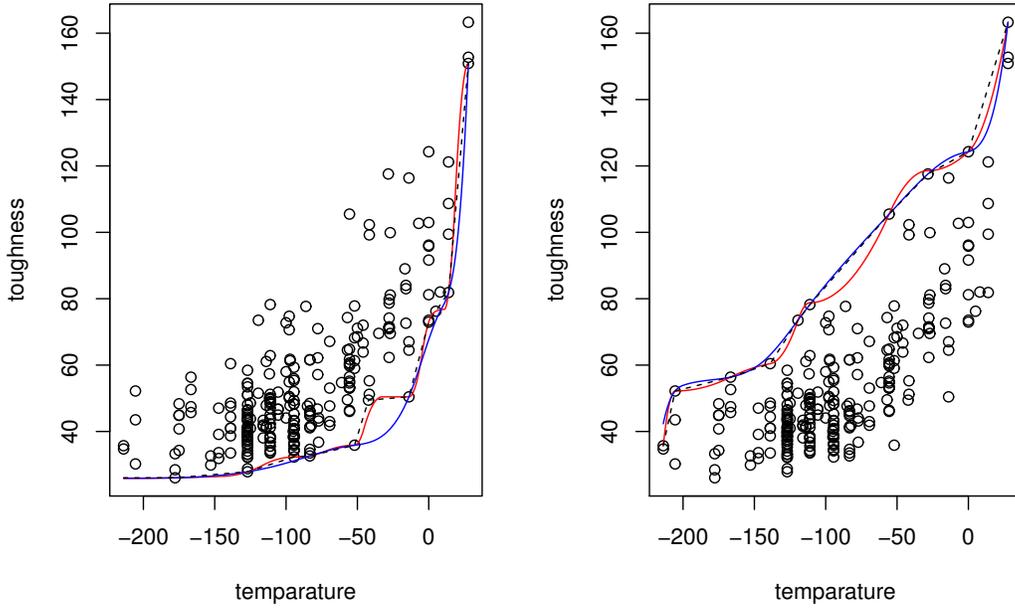
Figure 5: Scatterplot of the 254 nuclear reactors data, with three frontier estimates: LFDH (dotted black), QS-A (solid red) and CS-A (solid blue). From left to right, the estimates for the lower and the upper support boundaries.
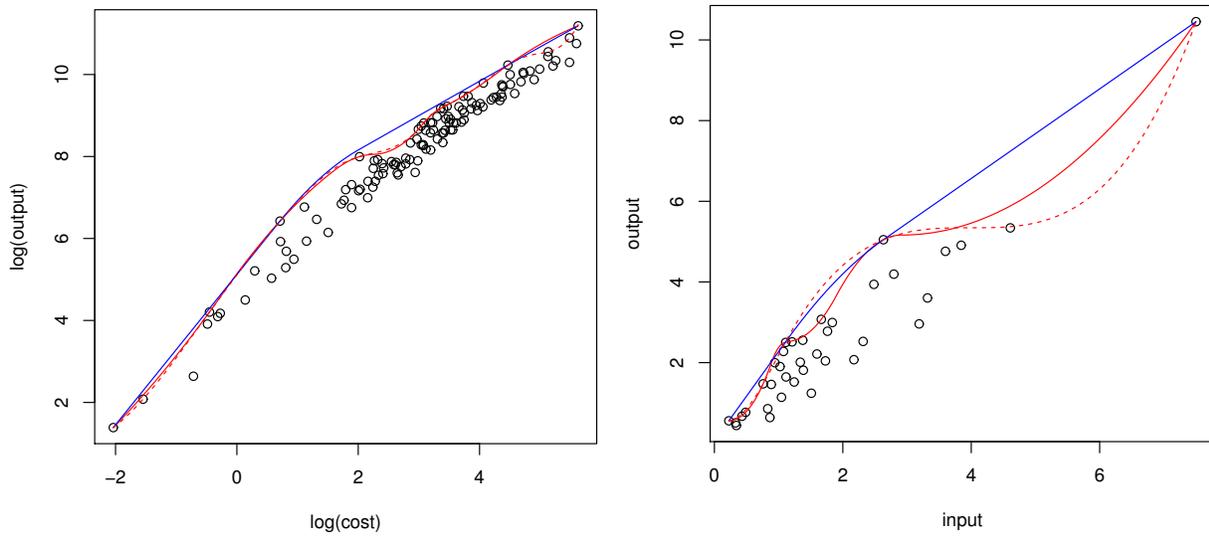
Figure 6: Scatterplots of the 123 American electric utility companies' data and the 37 European Air Controllers' data with three estimates of the efficient extremity in each plot: QS-A (solid red), CS-A (dotted red) and QS-C (solid blue)